Journal of Rock Mechanics and Geotechnical Engineering 15 (2023) 169–178

Contents lists available at ScienceDirect

Journal of Rock Mechanics and Geotechnical Engineering

journal homepage: www.jrmge.cn

Full Length Article

Analyses of non-aqueous reactive polymer insulation layer in high geothermal tunnel

Yu Chen [a], Shiyu Wang [a], Chengchao Guo [a,b], Cungang Lin [a,*], Chenyang Zhao [a]

[a] School of Civil Engineering, Sun Yat-sen University, Zhuhai, 519082, China
[b] Southern Institute of Infrastructure Testing and Rehabilitation Technology, Huizhou, 516000, China

ARTICLE INFO

Article history:
Received 12 October 2021
Received in revised form
10 December 2021
Accepted 20 January 2022
Available online 1 April 2022

Keywords:
Geothermal tunnel
Non-aqueous reactive polymer
Thermal conductivity
Heat insulation

ABSTRACT

The scenario of geothermal tunnel is commonly observed around the world, and increases with the new constructions in the long and deep tunnels, for example in China. Tunnel insulation is generally divided into active and passive insulation. In passive insulation, it is an effective way to set low thermal conductivity materials as the thermal insulation layer as the choice of insulation material mainly depends on the thermal conductivity. Polymer is a kind of material with good geothermal performance, but there are relatively few studies. In this context, the transient plane source (TPS) method was used to measure the thermal conductivity of the developed polymer. Then, the temperature field of the high geothermal tunnel insulated by the non-aqueous reactive polymer layer was simulated. With the parametric analysis results, the suggestions for the tunnel layers were proposed accordingly. It revealed that the thermal conductivity of polymer first increases and then decreases with temperature. There are two rising sections (−40–10 °C and 20–90 °C), one flat section (10–20 °C) and one descending section (>90 °C). It is observed the thermal conductivity of polymer increases with increase of the density of insulation layer and the density, and the thermal conductivity decreases when exposed to high temperatures. The temperature of the surrounding rocks increases with increase of the thermal conductivity and the thickness of polymer. Finally, a more economical thickness (5 cm) was proposed. Based on the parametric study, a thermal insulation layer with thermal conductivity less than 0.045 W/(m K), thickness of 5 cm and a density less than 0.12 g/cm^3 is suggested for practice.

1. Introduction

In construction of the tunnels, many long and deep tunnels that pass through the regime with active geological structures and high geo-temperature are frequently reported (Xian, 1997; Kairong, 2017; Deng et al., 2019). High geothermal scenario has significant impacts on the construction and operation of the tunnels:

(i) When selecting suitable materials, it is necessary to consider its reliability against high-temperature environments, for example the high geothermal resistant capacity;
(ii) High temperature leads to cracks in the concrete structure lining. From a long-term perspective, structural cracks can often lead to concentrated stresses and reduced structural durability; and
(iii) The mechanical equipment was severely affected with reduced conversion efficiency. The possibility of failures gradually increased, and the construction progress of the project was dragged down (Jing, 2012).

For potential materials, thermal conductivity of the target material is of priority. In terms of thermal conductivity, Gustafsson et al. (1979) first proposed the transient hot-strip method. The thermal conductivity can be roughly estimated by the curve of the apparent initial resistance and the square of the heat flow. In 1991, the transient hot-strip method was extended to the transient plane source (TPS) method (Gustafsson, 1991) and its performance was verified in 1995 (Log and Gustafsson, 1995). Many scholars use the TPS method to test the thermal conductivity of materials (Agrawal et al., 2015; Laguela et al., 2015; Shah et al., 2015; Zhang et al., 2015a,b) and study the factors that affect thermal conductivity, such as material density, ambient temperature (Zhang et al.,

* Corresponding author.
E-mail address: lincg@mail.sysu.edu.cn (C. Lin).
Peer review under responsibility of Institute of Rock and Soil Mechanics, Chinese Academy of Sciences.

https://doi.org/10.1016/j.jrmge.2022.01.013

2015a,b; Mendes et al., 2016; Adamoviet al., 2020). The thermal conductivity will increase with increase of the water content (Xiao et al., 2009) and the temperature (Zhang et al., 2020). However, for the polymer applied to rock tunnels, its parametric analyses are insufficient.

Materials with low thermal conductivity are widely used in the field of heat insulation. In high geothermal tunnel, the insulation layer can be installed to isolate the transmission of high rock temperature to the inside of the tunnel. Accordingly, the temperature inside the tunnel could be controlled within an acceptable range. Some scholars analyze numerically the temperature field of a tunnel with a thermal insulation layer (e.g. Zhou et al., 2015, 2021; Li et al., 2016; Wu and Wang, 2017; Zheng et al., 2020). There are many kinds of tunnel insulation materials available for practice, such as thermal insulation gunite (Wang et al., 2020), thermal insulation concrete material (Pang et al., 2016), and polyurethane boards (Li et al., 2020a). The above-mentioned materials can prevent heat transfer and the efficiency is limit.

However, studies on the thermal conductivity of non-aqueous reactive two-component polymer material that can be applied to the tunnel insulation layer are not rare. In this paper, the thermal insulation properties of the polymer were analyzed and its application to high geothermal tunnel insulation was discussed. The TPS method was used to measure the thermal conductivity of the polymer. In addition, the temperature field of the high geothermal tunnel insulated by the non-aqueous reactive polymer layer was simulated. Finally, some suggestions were provided for the tunnel geothermal layers in practice.

2. Measurement of thermal conductivity of polymer based on TPS method

2.1. Test method

The TPS method (Gustafsson et al., 1979, 1986; Gustafsson, 1991) utilizes a thin disk-shaped temperature-dependent resistor as the temperature sensor and heat source simultaneously for measurements of the thermal conductivity (λ) and thermal diffusivity (α). The sensor is sandwiched between two specimen halves, as indicated in Fig. 1. By recording the voltage variation and the current variation over a certain time period from the onset of the heating current, it is possible to obtain information on the heat flow between the sensor and the test specimen. By measuring the thermal conductivity (λ) and thermal diffusivity (α) of the test specimen, the volumetric heat capacity can be drawn as $\rho c = \lambda/\alpha$, where ρ is the density of the test specimen and c is the specific heat capacity of the test specimen (see Fig. 2).

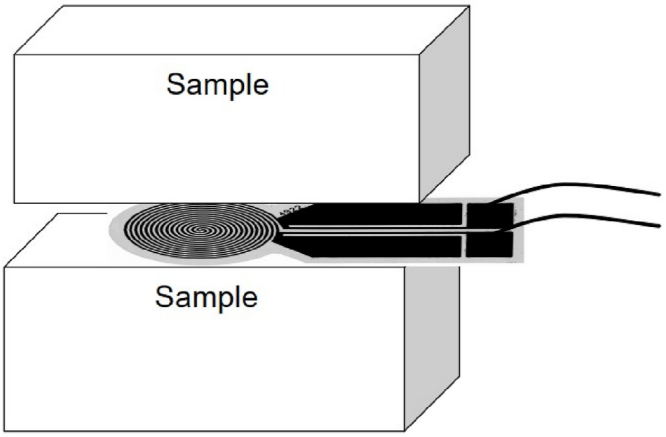

Fig. 1. Principal experimental set-up for the TPS method (Log and Gustafsson, 1995).

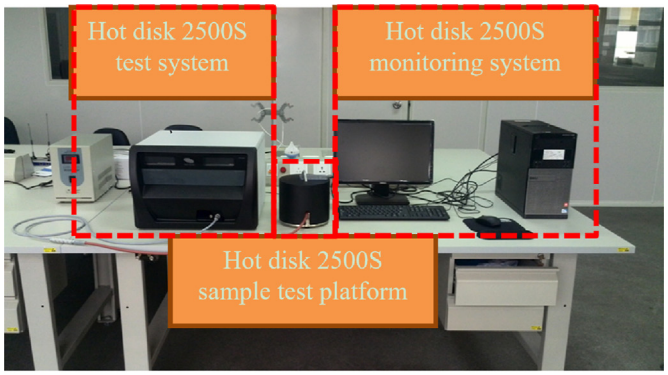

(a)

(b)

Fig. 2. Test equipment and sample placement position: (a) The test equipment (Hot Disk 2500S) and (b) The test specimen.

Under the constant power, the resistance of the probe changes with time:

$$R(t) = R_0\,(1 + k\Delta T) \tag{1}$$

where t is the testing time, R_0 is the probe initial resistance, k is the temperature coefficient of resistance, and ΔT is the average temperature rise of probe surface.

$$\Delta T(\tau) = \frac{P_0}{\left(\frac{3}{2}\pi r\lambda\right)} D(\tau) \tag{2}$$

where P_0 is the constant power, r is the probe radius, and $D(\tau)$ is the dimensionless function of characteristic time $\tau = \sqrt{at}/r$.

The thermal conductivity (λ) can be drawn by recording probe temperature ΔT and by fitting $D(\tau)$. In order to verify the data when

Table 1
The parameters used for the specimens.

Specimen size ($\Phi \times H$) (mm × mm)	Theoretical density (g/cm^3)	Measured density (g/cm^3)
79.8 × 20	0.05	0.07
	0.2	0.12
	0.3	0.24
	0.4	0.3
79.8 × 30	0.05	0.07
	0.2	0.12
	0.3	0.24
	0.4	0.3
79.8 × 40	0.05	0.07
	0.2	0.12
	0.3	0.24
	0.4	0.3

fitting a line, the depth of detection $D = 2\sqrt{\alpha t}$ (mm) can be used. When fitting the data, it should be ensured that the heat generated during the measurement process is not transferred outside the boundary of the sample, i.e. $D < r$.

2.2. Test equipment

The test equipment (Hot Disk 2500S) at the School of Civil Engineering of Sun Yat-sen University was used to conduct the thermal conductivity measurement tests. The testing output power is 25 mW and the testing time is 320 s. The probe model is Kapton 8563 with a radius of 9.868 mm. Such test is based on Fourier's one-dimensional heat transfer law, which refers to as the amount of heat conduction through a given cross-section per unit time in the heat conduction process. It is proportional to the temperature change rate and the cross-sectional area in the direction perpendicular to the cross-section. The direction of heat transfer is opposite to the direction of temperature rise, which can be used to calculate the amount of heat conduction and the thermal conductivity afterwards.

2.3. Sample preparation

The developed material used in this study is a non-aqueous reactive polyurethane material. Such non-aqueous reactive

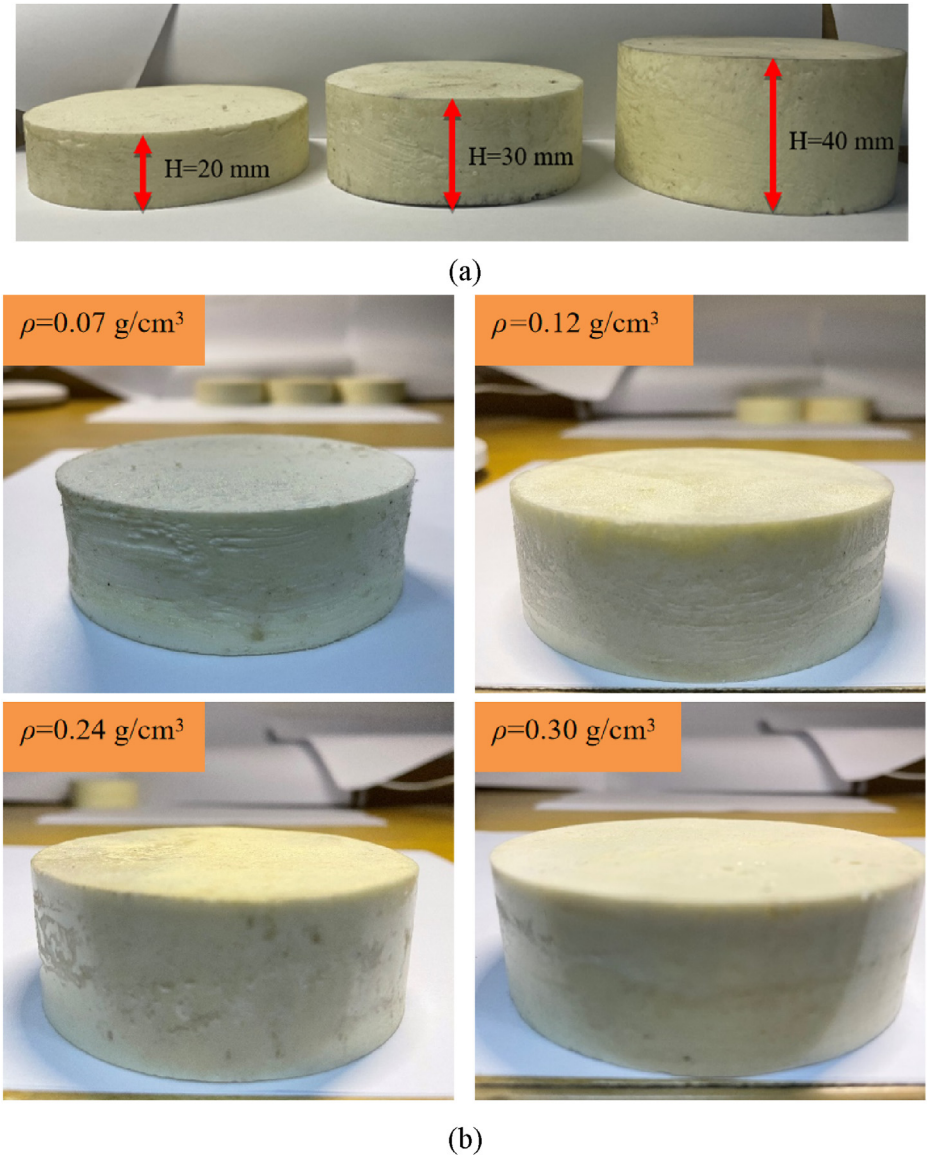

Fig. 3. The Polymer samples with different thicknesses and densities: (a) Different thicknesses and (b) Different densities.

polyurethane is a two-component foamed polyurethane polymer material formed by the reaction of isocyanate and polyol. According to the specification (GB/T 32064-2015, 2015), the effective diameter of the test surface of the sample should not be less than twice the diameter of the probe, and the thickness of the bulk sample should be greater than the selected probe diameter, not less than the probe radius. The specific specimen parameter is shown in Table 1 and the samples are shown in Fig. 3. Ten samples of different densities and three groups of samples with different thicknesses are prepared, totaling 120 samples. The polymer spraying equipment was used for the sample preparation. The foam volume of the polymer increased during the process accordingly. It is the reason why there is difference between the theoretical density and the measured density in Table 1. In addition, the scanning electron microscope (SEM) images in Fig. 4 on the polymer display that the polymer has a porous closed-cell structure (Li et al., 2020a). Fig. 4 shows the microstructure of the polymer, and four densities (0.1 g/cm^3, 0.244 g/cm^3, 0.5 g/cm^3, 0.732 g/cm^3) are used for tests. The higher the density, the smaller the microparticle diameter of the polymer. Such structure characteristic makes the polymer denser and stronger. In this paper, the density of 0.732 g/cm^3 is selected for the subsequent numerical simulations.

3. Influence of different factors on the thermal conductivity of polymer

The polymer has a closed-cell structure and small pore size, as displayed in Fig. 4. This means that the polymer material has excellent thermal insulation performance. There are many factors affecting its thermal conductivity, such as ambient temperature, water content, porosity, density, heat flow direction. The closed-cell structure of the polymer gives it extremely high-water vapor barrier performance and significant water impermeability. As it is difficult to control the porosity during sample preparation, only the ambient temperature and material density are considered.

3.1. Influence of ambient temperature on the thermal conductivity of polymer

The ambient temperature changes from -40 °C to 100 °C and the thermal conductivity is measured at an interval of 10 °C. Afterwards, the test was reset to the initial state. The same test condition was carried out for 3 times with an interval of about 5 min of each test. In order to complete the tests efficiently, the temperature was artificially cooled to ensure that it dropped to the initial temperature during this stage. Such artificial cooling measures within 5 min were enough to ensure that the probe restored to the initial stage. The thermal conductivity results of the polymer samples with a measured density of 0.07 g/cm^3 are shown in Table 2. The results of the thermal conductivity of polymers with different densities at different temperatures are shown in Fig. 5.

The thermal conductivity of polymer materials increases first and then decreases with increase of the temperature, as shown in Fig. 5. However, there is a gentle section in the range of 10–20 °C. Based on these phenomena, the increasing process can be divided into two stages: −40–10 °C and 20–90 °C. The increasing rate of thermal conductivity in the latter stage is 1.12 times that of the previous one.

For the stages of −40–10 °C and 20–90 °C, there will be a temperature difference between the inside and outside parts of the polymer cell when the temperature rises. There is thermal acceleration of gas and solid molecules, which induces the increase of the value of thermal conductivity. The higher the temperature, the more violent the random movement of gas molecules and the faster the thermal conductivity drops. In the smooth section of 10–20 °C and at the point of 90 °C, the external environment and the inside of the polymer cell form a thermal equilibrium. At this moment, the

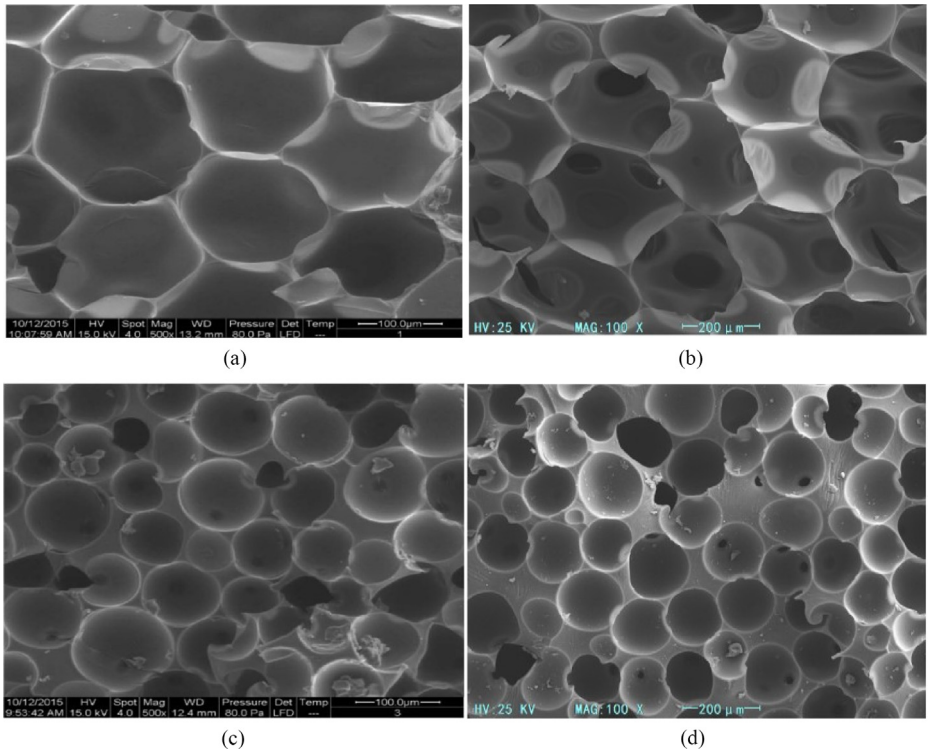

Fig. 4. Polymer SEM images: (a) ρ = 0.1 g/cm^3; (b) ρ = 0.244 g/cm^3; (c) ρ = 0.5 g/cm^3 and (d) ρ = 0.732 g/cm^3.

Table 2
Thermal conductivity of polymers at different temperatures (ρ = 0.07 g/cm^3).

Temperature (°C)	First test W/(m K)	Second test (W/(m K))	Third test (W/(m K))	Average (W/(m K))
-40	0.02397	0.02359	0.02366	0.02374
-30	0.02419	0.02408	0.02406	0.02411
-20	0.02437	0.02444	0.02428	0.02436
-10	0.02482	0.02488	0.02472	0.02481
0	0.02483	0.02487	0.02475	0.02482
10	0.02509	0.025	0.02475	0.02495
20	0.02533	0.02535	0.02514	0.02527
30	0.02628	0.02624	0.02607	0.02619
40	0.02763	0.02756	0.02718	0.02746
50	0.02933	0.02925	0.02911	0.02923
60	0.0304	0.03032	0.0301	0.03027
70	0.03129	0.0312	0.03096	0.03115
80	0.03208	0.032	0.03177	0.03195
90	0.03316	0.033	0.03278	0.03298
100	0.03166	0.03261	0.0329	0.03239

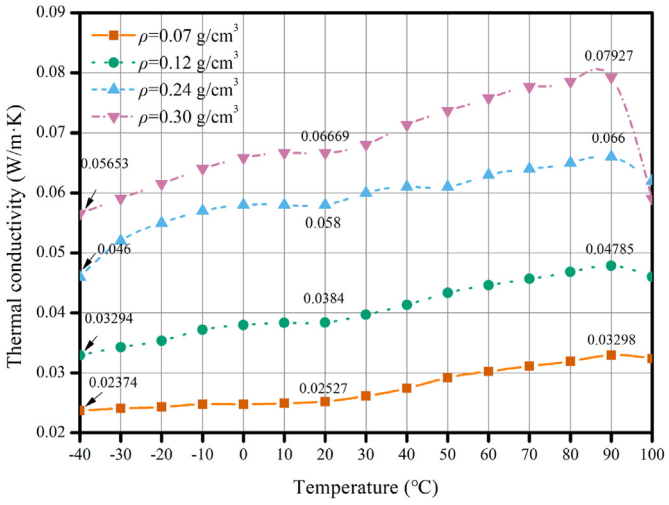

Fig. 5. Variation of thermal conductivity of polymers with different densities and different temperatures.

thermal conductivity increases slowly and reaches the maximum value at 90 °C (Fig. 6). The thermal conductivity starts to reduce at 100 °C and this phenomenon occurs in all test samples in this series. It may be because the temperature is high and a large number of gas molecules in the pores move violently. There is a small amount of moisture inside the sample during the sample preparation process and the moisture evaporates at 100 °C normally.

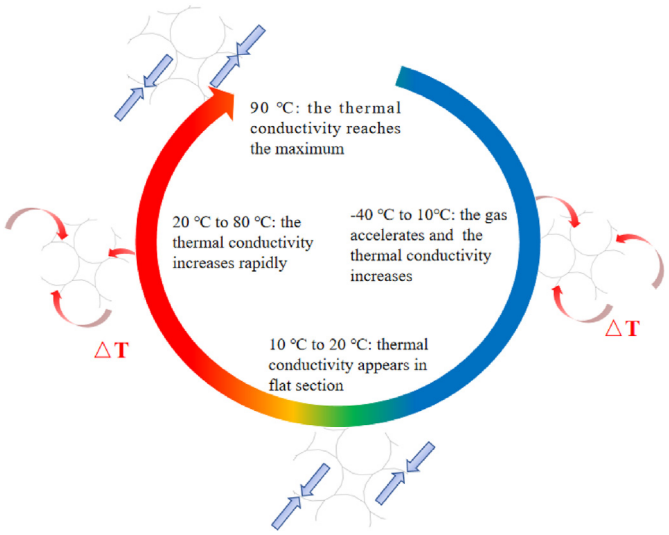

Fig. 6. The mechanism of temperature influence on thermal conductivity of polymer.

3.2. Influence of material density on the thermal conductivity of polymer

The density of the polymer material was measured before the test. In order to represent the practical condition in site, the spraying technique was carried out on the tunnel surface. The cylinder-shaped specimens were obtained directly from the polymer spray layer. Such a technique may cause the measured density of the sample to be inconsistent with the theoretical density because the upper and lower surfaces of the sample were free to expand and there was no confining pressure when the sample was made. It is defined that the measured density values (0.07 g/cm^3, 0.12 g/cm^3, 0.24 g/cm^3 and 0.3 g/cm^3) corresponding to theoretical density (0.05 g/cm^3, 0.1 g/cm^3, 0.3 g/cm^3 and 0.4 g/cm^3) in this study. According to the current research on the fine microstructure of polymer by our research group in Fig. 7 (Wei et al., 2017; Li et al., 2020b), with increasing density, the density of the polymer is greater, the microstructure is denser and the cell diameter is smaller. The test results are shown in Table 3 and Fig. 8.

When the temperature is low, the thermal conductivity of polymer shows an increasing trend with increase of the density. For every increment of 1 g/cm^3 in density, the thermal conductivity increases by 0.1709 W/(m·K). At higher temperatures, the thermal conductivity of polymers increases first and then decreases with increase of the density (Fig. 8).

Polymer is porous and closed-cell material. The porosity, cell diameter and the amount of air in the pores show a decreasing trend as the density increases (Fig. 7). The thermal conductivity of air is 0.023 W/(m K) and the thermal conductivity of polymer materials is close to the thermal conductivity of air when density is small. When the temperature reaches 100 °C and ρ > 0.24 g/cm^3, the intensity of convective heat transfer increases, the random movement of gas molecules is enhanced and the violent and irregular movement of gas molecules consumes a lot of heat.

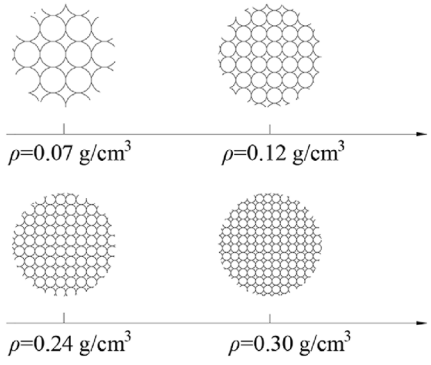

Fig. 7. Polymer microstructure changes with density.

Table 3
Thermal conductivity of polymer with the same material density (20 °C).

Measured density (g/cm^3)	First test	Second test	Third test	Average
0.07	0.02533	0.02535	0.02514	0.02527
0.12	0.0386	0.03831	0.03829	0.0384
0.24	0.055	0.054	0.055	0.055
0.3	0.06733	0.06605	0.06669	0.06669

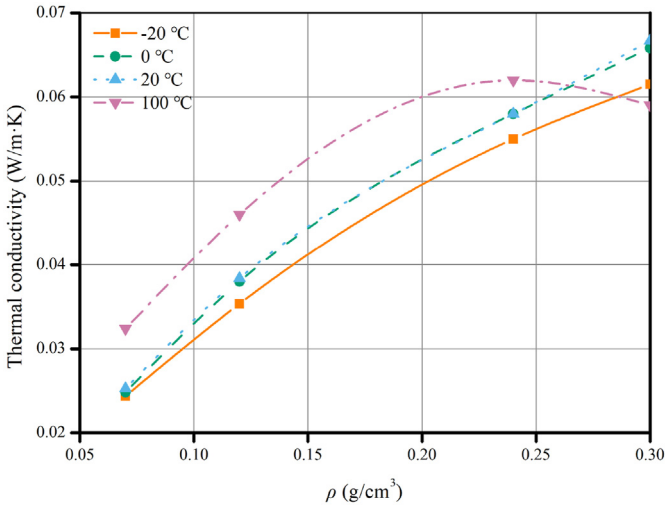

Fig. 8. Variation of thermal conductivity of polymers with density.

Therefore, when the density increases, the thermal conductivity decreases at 100 °C. In addition, the values of the material porosity, the cell diameter and the amount of air are small, which induces the thermal conductivity to decrease with increase in the density. In other words, the thermal conductivity decreases with the increasing density in certain temperature conditions. It should be noted that the optimal density corresponding to different practical engineering conditions can be suggested.

3.3. Comparison of non-aqueous reactive polymer and traditional thermal insulation materials

Over the last decades, many tunnels in China were constructed with a shallow depth; therefore, high rock temperature was rarely encountered. With the increasing number of deep, long, and large tunnels, the problem of thermal damage has gradually become a challenge in tunnel construction. In order to prevent heat damage, passive cooling measures are often adopted. Some materials with better thermal insulation properties are used in the tunnel to prevent the transfer of thermal insulation from the surrounding rocks to the concrete lining.

The choice of thermal insulation material is critical to the effect of thermal insulation performance, and the index to measure thermal insulation performance of such material is the thermal conductivity. The lower the thermal conductivity, the better the thermal insulation performance. Insulation materials commonly used in tunnel engineering include aluminum silicate fibers, extruded polystyrene foam materials, vitrified microbead insulation mortar, expanded polystyrene and polycarbonate. During the practical spraying construction, the non-aqueous reactive polymer can form quickly and the bonding strength is sufficient to meet the requirements of the construction site. A detailed comparison of the main indicators of traditional tunnel insulation materials and non-aqueous reactive polymer is shown in Table 4 (Wei et al., 2017).

4. Numerical simulation of high geothermal tunnel with non-aqueous reactive polymer insulation layer

4.1. Model building

Since the heat transfer in the axial direction of the tunnel is much smaller than the heat transfer in radial direction, the tunnel is simplified into a two-dimensional (2D) calculation. The tunnel is composed of 25 cm concrete primary support, 5 cm polymer insulation layer and 45 cm concrete secondary lining. The depth of the tunnel is 43.73 m, the tunnel radius is 5.45 m and the model has a dimension of 100 m × 100 m. The outer boundary is five times the tunnel radius, which ensures no boundary effect occurs. The model uses the PLANE55 unit, in which the mesh size of the primary

Table 4
Performance index of thermal insulation material (Wei et al., 2017).

Performance parameter	Non-aqueous reactive polymer	Expanded polystyrene foam	Fulikai Insulation Board	Phenolic foam	Rigid PVC foam	Rock wool	Dry-process aluminum silicate fiber material
Density (g/cm^3)	0.045	0.04	0.05	0.05	0.13	0.061–0.2	0.188
Thermal conductivity (W/m $ k)	0.018–0.024	0.041	0.026–0.033	0.03	0.04	≤0.044	0.037
Specific absorption of volume (%)	≤1	≤4	≤7	≤3.7	≤4	≤5	–
Operating temperature range (°C)	−60–120	−80–75	−196–300	−180–150	−30–400	≤600	≤1000
Freezing resistance	No embrittlement or shrinkage at low temperature	Low temperature resistance	No deformation, cracking, or brittleness			No cracks, no peeling	No deformation, cracking, or brittleness
Compressive strength (MPa)	≥0.2	≥0.06	≥0.2	≥0.25	0.15	0.107	0.5
Burning performance	Flame-retardant	Temperature <75 °C	Non-combustible	Non-combustible	Not flammable	Not flammable	Non-combustible

Table 5
The parameters of the materials of the model.

Material	Thickness (cm)	Density (g/cm^3)	Thermal conductivity (W/(m K))	Specific heat capacity (J/(kg °C))	Poisson's ratio, υ	Elastic modulus (GPa)	Cohesive forces (MPa)	Angle of internal friction (°)
Surrounding rocks	–	2	2.3	707	0.4	1.2	0.1	24
Primary support	25	2.2	2.94	960	0.2	23	–	–
Secondary lining	45	2.5	2.94	960	0.2	32.5	–	–
Polymer insulation layer	5	0.045	0.024	180	0.2	0.15	0.14	21.85

support, secondary lining and the polymer insulation layer is 0.1 m, and the size of the surrounding rock is 1 m. The material of each part is shown in Table 5. The heat conduction among the surrounding rocks, primary lining and second lining follows Fourier's one-dimensional heat transfer law, $\boldsymbol{q} = -\boldsymbol{k}\mathrm{d}T/\mathrm{d}x$. The symbol $\boldsymbol{q}$ is the heat flux, which is the heat per unit area, and it is a vector. $\mathrm{d}T/\mathrm{d}x$ is the thermal gradient in the direction of the flow. The minus sign is to show that the flow of heat is from hotter to colder. If the temperature decreases with axial distance x, $\boldsymbol{q}$ will be positive and will flow in the direction of x. If the temperature increases with x, $\boldsymbol{q}$ will be negative and will flow opposite to the direction of x.

4.2. Boundary and loading conditions

In the thermal simulation of ANSYS, the interface is virtual between the insulation layer and primary/second lining (see Fig. 9). This interface is not necessary to be specifically defined as it is not applied for the mechanical loading transfer, but only applied for the heat transfer. The initial surrounding rock temperature is set to 60 °C for numerical model. According to the specification, the temperature in the tunnel shall not exceed 28 °C, and thus the initial temperature of the lining layer is set to 28 °C. The initial temperature field of the transient thermal analysis is shown in Fig. 10.

By applying convective heat transfer conditions on the inner side of the secondary lining of the tunnel, the ambient temperature is set to 28 °C, and the convective heat transfer coefficient is set to 20 W/(m^2 °C).

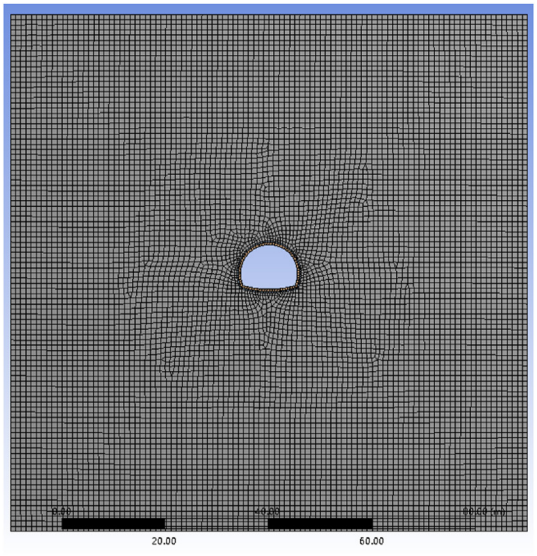

(a)

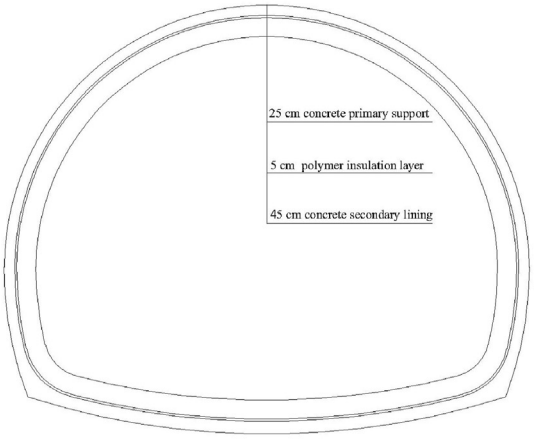

(b)

Fig. 9. Tunnel model: (a) The mesh and boundary condition of tunnel model and (b) The geometry of tunnel.

4.3. Influences of different polymer thermal insulation layer parameters on tunnel temperature field

4.3.1. Influence of thermal conductivity of thermal insulation layer material on tunnel temperature field

Thermal conductivity is a key factor when selecting the material used for the polymer heat insulation layer. The lower the thermal conductivity reveals the weaker the thermal conductivity. In order to ensure the reliability of the model output results for practical projects, the monitoring time of the model is 365 d. The relationship between the thermal conductivity and the support effect is not considered. In this study, the values of thermal conductivity (0.024 W/(m K), 0.035 W/(m K), 0.04 W/(m K), 0.06 W/(m K), 0.08 W/(m K), 0.1 W/(m K), 0.12 W/(m K), and 0.17 W/(m K) have been selected for simulation and the results are shown in Figs. 11 and 12. It shows that the larger the thermal conductivity, the larger the radius of the surrounding rock heat regulation circle. As the thermal conductivity increases, the heat conduction of the insulation layer strengthens, and the heat of the surrounding rocks can be released, resulting in larger radius of the heating ring.

In Fig. 11, '0 m' is the outermost point of the primary support of the model. On the basis of this point, different data points in the surrounding rocks are taken at regular intervals. There are three intervals in Fig. 11. In the interval of 0.02–0.045 W/(m K), the temperature of the surrounding rocks increases by 0.211 °C for every increment of 0.001 W/(m K) in the thermal conductivity. This stage is a highly efficient heat insulation zone. In the interval of 0.045–0.1 W/(m K), the temperature of the surrounding rocks increases by 0.123 °C for every decrease of 0.001 W/(m K) in the thermal conductivity. This interval is a general heat insulation zone. In the interval of 0.1–0.17 W/(m K), the temperature of the surrounding rocks increases by 0.021 °C for every decrease of 0.001 W/(m K) in the thermal conductivity. Therefore, this interval is a low-efficiency heat insulation zone.

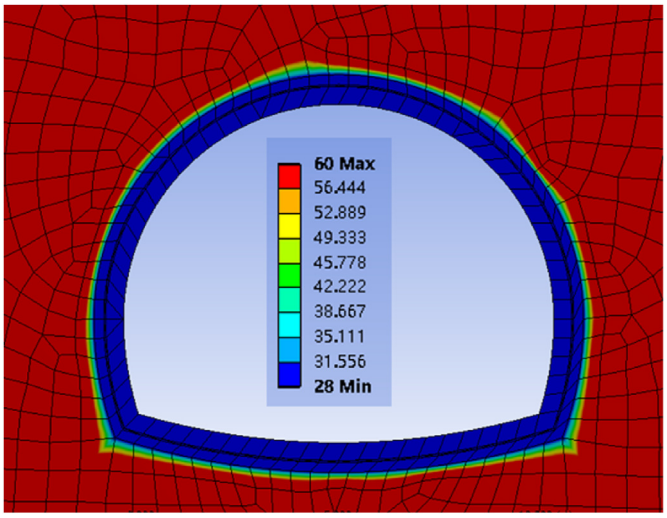

Fig. 10. The initial temperature field of the transient thermal analysis.

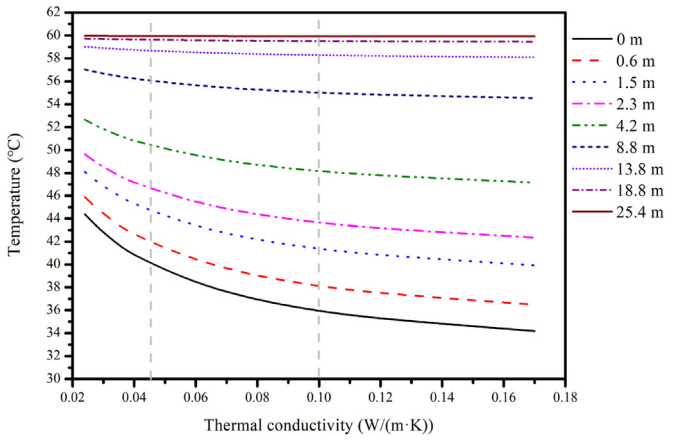

Fig. 11. Variations of temperature at different depths of surrounding rocks with different thermal conductivities.

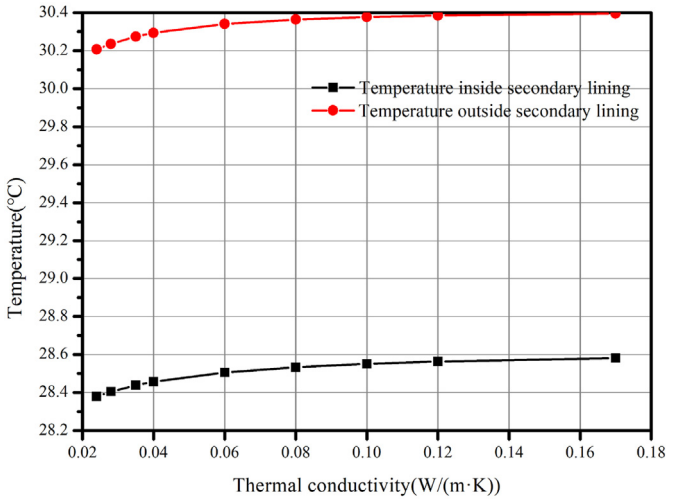

Fig. 12. The temperature distribution inside and outside the secondary lining changes with the thermal conductivity.

When the thermal insulation layer is sandwiched, the change of thermal conductivity has slight effect on the temperature change inside the tunnel, but thermal insulation materials with thermal conductivity in the high-efficiency thermal insulation zone are the best. With increase of the thermal conductivity, the temperatures inside and outside the secondary lining of the tunnel increase, and both appear to be faster at the beginning and tend to be flat afterwards in Fig. 12. The smaller the thermal conductivity, the lower the temperature of the secondary lining. Such a phenomenon can effectively improve the stress conditions of the secondary lining.

4.3.2. Influence of thickness of the thermal insulation layer on tunnel temperature field

In this study, eight cases of numerical simulations are carried out with different thicknesses of the thermal insulation layer (e.g. 0 cm, 3 cm, 4 cm, 5 cm, 8 cm, 10 cm, 15 cm, and 25 cm), as shown in Figs. 13 and 14.

There are also three intervals in Fig. 13. For thickness of 0–5 cm, the insulation effect of the first zone is obvious. For every 1 cm increase in the thickness of the thermal insulation layer, the

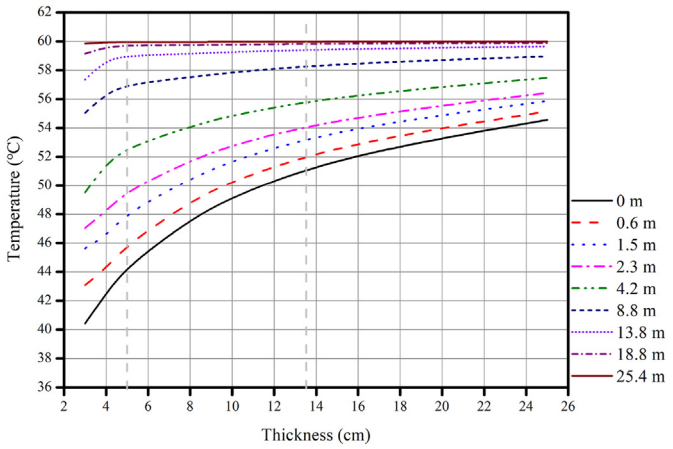

Fig. 13. The temperature variation at different depths of surrounding rocks with thickness of the insulation layer.

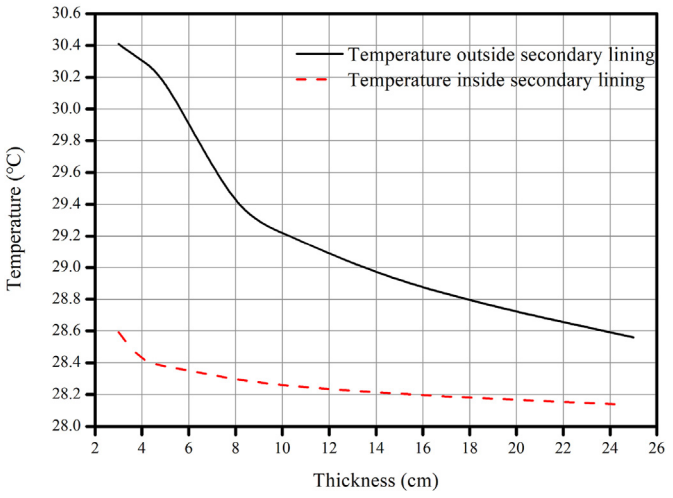

Fig. 14. The temperature variation inside and outside the secondary lining with the thickness of the insulation layer.

surrounding rock temperature increases by about 2 °C, which is an efficient heat insulation zone. When the thickness is 10 cm, the slopes of most curves are relatively large, and when the thickness reaches 20 cm, the slopes tend to be flat. In some practical projects, 5 cm is generally used as a measurement interval. Therefore, 15 cm is set as the boundary of an interval, which is convenient for field monitoring and analysis. For thickness between 5 cm and 15 cm, for every 1 cm increase in the thickness of the thermal insulation layer, the surrounding rock temperature will increase by about 1 °C, which is a general heat insulation zone. For thickness between 15 cm and 25 cm, for every 1 cm increase in the thickness of the thermal insulation layer, the surrounding rock temperature will increase by about 0.33 °C, which is an inefficient heat insulation zone.

According to the results of most temperature calculations, it is obvious that there are turn points for most curves when the thickness is 5 cm. Beyond 5 cm, the rising trend of many curves becomes mild. It is necessary to significantly increase the thickness of polymers in order to have insulation performance. In addition, it is also easy to understand that it will take more cost to get the same

effect beyond 5 cm. Therefore, this paper suggests that the preliminarily spraying thickness of polymer is 5 cm.

4.4. Reasonable suggestions for polymer insulation layer

According to the measurements of thermal conductivity of polymer-based on TPS technique, the thermal conductivity is smaller than 0.05 W/(m K), and the polymers with a density of 0.07 g/cm^3 and 0.12 g/cm^3 are applicable at −40–100 °C. Polymers with a density greater than 0.12 g/cm^3 cannot meet the requirements. Based on the numerical simulations, 0.02–0.045 W/(m K) is the high-efficiency heat insulation zone, therefore, the thermal conductivity should be selected less than 0.045 W/(m K), and 5 cm is the optimum thickness for the polymer heat insulation layer.

In summary, a thermal insulation layer with thermal conductivity less than 0.045 W/(m K), thickness of about 5 cm and a density less than 0.12 g/cm^3 should be selected. To some extent, the non-aqueous reactive polymer can be applied to rock tunnel projects and replace the traditional thermal insulation materials. In addition, the waterproof and energy-absorption functions have attracted research interest due to the potential advantages for tunnel construction.

5. Conclusions

According to the plane TPS method, Hot Disk 2500S was used to test the thermal conductivity of the developed polymers. A numerical model was established by using ANSYS to simulate the tunnel ventilation using applied convective loads. In this context, the temperature field changing laws of the tunnel under different thermal conductivities and different thicknesses of the polymer thermal insulation layer are studied.

(1) The thermal conductivity of polymer materials first increases and then decreases with increase of the ambient temperature. There is a gentle section in the range of 10–20 °C. The increasing process is −40–10 °C and 20–90 °C, and the increase rate of thermal conductivity in the latter stage is 1.12 times that of the previous stage. When temperature is larger than 90 °C, the thermal conductivity decreases rapidly.
(2) The temperature of surrounding rocks increases with increase of the thermal conductivity. When the thermal conductivity is lower than 0.045 W/(m K), the heat insulation effect is optimum, and the density of the polymer material should be selected less than 0.12 g/cm^3.
(3) The temperature of surrounding rocks rises with the increase of thickness. When the thickness is about 5 cm, the heat insulation effect is optimum.

The developed polymer material is a kind of material with a predominant thermal insulation effect. It can be used as a thermal insulation layer in tunnels, providing a reference for tunnel thermal insulation material selection.

Declaration of competing interest

The authors declare that they have no known competing financial interests or personal relationships that could have appeared to influence the work reported in this paper.

Acknowledgments

The research was funded by the research and development program of China State Railway Group Co., Ltd. (Grant Nos. K2019G032 and P2019G040) and the program for Guangdong Introducing Innovative and Enterpreneurial Teams (Grant No. 2016ZT06N340).

References

Adamovic, T., Veselinovi, V., Trtic, N., et al., 2020. Mechanical properties of new denture base material modified with gold nanoparticles. J. Prosthodont. Res. 65 (2).
Agrawal, R., Saxena, N.S., Sreekala, M.S., Thomas, S., 2015. Effect of treatment on the thermal conductivity and thermal diffusivity of oil-palm-fiber-reinforced phenolformaldehyde composites. J. Polym. Sci. B Polym. Phys. 38 (7), 916–921.
Deng, J., Lei, C.K., Yang, X., Li, M., Wang, K., Shu, C.M., 2019. The effect of high geo-temperature environment on coal spontaneous combustion: an experimental study. In: Proceedings of the 11th International Mine Ventilation Congress, pp. 539–551, 2019.
GB/T 32064-2015, 2015. Determination of Thermal Conductivity and Thermal Diffusivity of Building Materials: Transient Plane Heat Source Method. Ministry of Housing and Urban-Rural Development, China.
Gustafsson, E.S., 1991. Transient plane source techniques for thermal conductivity and thermal diffusivity measurements of solid materials. Rev. Sci. Instrum. 62 (3), 797.
Gustafsson, S.E., Karawacki, E., Khan, M.N., 1979. Transient hot-strip method for simultaneously measuring thermal conductivity and thermal diffusivity of solids and fluids. J. Phys. D Appl. Phys. 12 (9), 1411–1421.
Gustafsson, S.E., Karawacki, E., Chohan, M.A., 1986. Thermal transport studies of electrically conducting materials using the transient hot-strip technique. J. Phys. D Appl. Phys. 19 (5), 727.
Jing, D., 2012. Study on high geothermal issue in deep-buried tunnel. Shanxi Architect. 38 (17), 196–197 (in Chinese).
Kairong, H., 2017. Development and prospects of tunnels and underground works in China in recent two years. Tunn. Constr. 2, 14–25.
Laguela, S., Bison, P., Peron, F., Romagnoni, P., 2015. Thermal conductivity measurements on wood materials with transient plane source technique. Thermochim. Acta 600, 45–51.
Li, M.J., Fang, H.Y., Du, M.R., Zhang, C., Su, Z., Wang, F.M., 2020a. The behavior of polymer-bentonite interface under shear stress. Construct. Build. Mater. 248, 118680.
Li, S., Niu, F., Lai, Y., Pei, W., Yu, W., 2016. Optimal design of thermal insulation layer of a tunnel in permafrost regions based on coupled heat-water simulation. Appl. Therm. Eng. 110, 1264–1273.
Li, Y., Wang, H., Yang, L., Su, S., 2020b. Study on water absorption and thermal conductivity of tunnel insulation materials in a cold region under freeze-thaw conditions. Adv. Mater. Sci. Eng. 2020, 5301968.
Log, T., Gustafsson, S.E., 1995. Transient plane source (TPS) technique for measuring thermal transport properties of building materials. Fire Mater. 19 (1), 43–49.
Mendes, M., Goetze, P., Talukdar, P., et al., 2016. Measurement and simplified numerical prediction of effective thermal conductivity of open-cell ceramic foams at high temperature. Int. J. Heat Mass Tran. 102, 396–406.
Pang, J.Y., Yao, W.J., Yao, W.J., 2016. Experimental research on performance of new type of thermal insulation concrete material in high geothermal tunnel. Chin. Concr. Cem. Prod. 1, 5–9.
Shah, D.U., Bock, M.C.D., Mulligan, H., Ramage, M.H., 2015. Thermal conductivity of engineered bamboo composites. J. Mater. Sci. 51 (6), 2991–3002.
Wang, J., Wan, Z., Zhang, H., Wu, D., Wang, G., 2020. Application of thermal insulation gunite material to the high geo-temperature roadway. Adv. Civ. Eng. 2020, 8853870.
Wei, Y., Wang, F., Gao, X., Zhong, Y., 2017. Microstructure and fatigue performance of polyurethane grout materials under compression. J. Mater. Civ. Eng. 29 (9), 0001954.
Wu, G., Wang, Z., 2017. Study on thermal insulation layer of high ground temperature railway tunnel. J. Railw. Sci. Eng. 14 (8), 1715–1726.
Xian, M., 1997. The main hole of the Abo Tunnel in Japan penetrates through the high-pressure water-bearing volcanic eruption layer and high temperature zone. Mod. Tunn. Technol. 1, 50–56.
Xiao, H., Cai, D., He, J., 2009. Measuring method of geomaterial thermal conductivity based on distributed optical fiber sensing technology. Chin. J. Rock Mech. Eng. 28 (4), 819–826.
Zhang, Q., Yuan, R., Zhu, G., Wang, X., 2020. Study on the influence of converter slag on thermal conductivity of pulverized coal. Energy Metall. Indust. 39 (2), 23–26.
Zhang, W., Min, H., Gu, X., Xi, Y., Xing, Y., 2015a. Mesoscale model for thermal conductivity of concrete. Construct. Build. Mater. 98, 8–16.

Zhang, W., Tong, F., Xing, Y., Gu, X., 2015b. Experimental study and prediction model of thermal conductivity of concrete. J. Build. Mater. 18 (2), 183–189.
Zheng, Y., Tao, L., Ye, X., et al., 2020. Temperature reduction for extra-long railway tunnel with high geotemperature by longitudinal ventilation. Tunn. Undergr. Space Technol. 99, 103381.
Zhou, X., Ren, X., Ye, X., Tao, L., Liu, X., 2021. Temperature field and anti-freezing system for cold-region tunnels through rock with high geotemperatures. Tunn. Undergr. Space Technol. 111 (3), 103843.
Zhou, X., Zeng, Y., Yang, Z., Zhou, X., 2015. Numerical solution of the heat transfer between tunnels and rocks in high geothermal geothermal region. J. Railw. Sci. Eng. 6, 1406–1411.

Dr. Yu Chen is an Associate Professor in the School of Civil Engineering at Sun Yat-sen University. He gained his BE and MSc at Central South University, China and PhD at the Norwegian University of Science and Technology, Norway. He has worked at Ramboll Consulting Denmark A/S and Central South University before. His research interests include rock mechanics, underground engineering, as well as numerical simulation in multi field-and-phase coupling.